



Climate change influences chlorophylls and bacteriochlorophylls metabolism in hypersaline microbial mat

Camille Mazière, M. Bodo, M.A. Perdrau, Cristiana Cravo-Laureau, Robert Duran, C. Dupuy, Cédric Hubas

► To cite this version:

Camille Mazière, M. Bodo, M.A. Perdrau, Cristiana Cravo-Laureau, Robert Duran, et al.. Climate change influences chlorophylls and bacteriochlorophylls metabolism in hypersaline microbial mat. *Science of the Total Environment*, 2022, 802, pp.149787. 10.1016/j.scitotenv.2021.149787. hal-03328597

HAL Id: hal-03328597

<https://hal.science/hal-03328597>

Submitted on 28 Jun 2023

HAL is a multi-disciplinary open access archive for the deposit and dissemination of scientific research documents, whether they are published or not. The documents may come from teaching and research institutions in France or abroad, or from public or private research centers.

L'archive ouverte pluridisciplinaire **HAL**, est destinée au dépôt et à la diffusion de documents scientifiques de niveau recherche, publiés ou non, émanant des établissements d'enseignement et de recherche français ou étrangers, des laboratoires publics ou privés.

Climate change influences chlorophylls and bacteriochlorophylls metabolism in hypersaline microbial mat

C. Mazière^{1,2*}, M. Bodo³, M. A. Perdrau², C. Cravo-Laureau¹, R. Duran¹, C. Dupuy², C. Hubas³

¹ Université de Pau et des Pays de l'Adour, E2S UPPA, CNRS, IPREM UMR 525 - Bât. IBEAS, BP1155, 64013 PAU cedex, France

² La Rochelle Université, CNRS, UMR 7266 LIENSs (Littoral Environnement et Sociétés)- 2, rue Olympe de Gouges, Bât. ILE, 17000 LA ROCHELLE, France

³ Muséum National d'Histoire Naturelle, UMR BOREA 8067, MNHN-IRD-CNRS-SU-UCN-UA - Station Marine de Concarneau, 29900 CONCARNEAU, France

* Corresponding author: camille.maziere@univ-pau.fr, +33 5 59 40 74 68, Bâtiment IBEAS – avenue de l'Université – 64013 Pau, France ; +33 5 46 50 76 31, Bâtiment Ile – 2, rue Olympe de Gouges – 17000 La Rochelle, France

Keywords: hypersaline microbial mats, ocean acidification, mesocosms, chlorophyll derivatives, phototrophic communities

Abstract

This study aimed to determine the effect of the climatic change on the phototrophic communities of hypersaline microbial mats. Ocean acidification and warming were simulated alone and together on microbial mats placed into mesocosms. As expected, the temperature in the warming treatments increased by 4°C from the initial temperature. Surprisingly, no significance difference was observed between the water pH of the different treatments despite of a decrease of 0.4 unit pH in the water reserves of acidification treatments. The salinity increased on the warming treatments and the dissolved oxygen concentration increased and was higher on the acidification treatments. A total of 37 pigments were

identified belonging to chlorophylls, carotenes and xanthophylls families. The higher abundance of unknown chlorophyll molecules called chlorophyll derivatives was observed in the acidification alone treatment with a decrease in chlorophyll *a* abundance. This change in pigmentary composition was accompanied by a higher production of bound extracellular carbohydrates but didn't affect the photosynthetic efficiency of the microbial mats. A careful analysis of the absorption properties of these molecules indicated that these chlorophyll derivatives were likely bacteriochlorophyll *c* contained in the chlorosomes of green anoxygenic phototroph bacteria. Two hypotheses can be drawn from these results: 1/ the phototrophic communities of the microbial mats were modified under acidification treatment leading to a higher relative abundance of green anoxygenic bacteria, or 2/ the highest availability of CO₂ in the environment has led to a shift in the metabolism of green anoxygenic bacteria being more competitive than other phototrophs.

1. Introduction

Since the industrial revolution, the atmospheric greenhouse gases concentration has increased sharply leading to a decrease in the pH of the surface ocean of about 0.1 pH unit (IPCC, 2014). In the coming decades, the ocean acidification will continue, associated with an ocean water warming caused by increasing levels of CO₂ in the atmosphere (Hutchins and Fu, 2017; IPCC, 2014). These climatic perturbations will alter the carbon and nutrients cycles on a global scale (Hutchins and Fu, 2017) and are expected to have a direct impact on all physical, chemical and biological parameters that govern marine organisms life (Hutchins and Fu, 2017). Organisms will be faced with unprecedented changes in future ocean conditions, particularly marine life will be severely affected. On France's Atlantic coasts, the Intergovernmental Panel on Climate Change (IPCC) predicts an increase in surface water temperature of 3 to 4 °C and ocean acidification of 0.4 to 0.45 pH units in its most pessimistic scenario (RCP 8.5) by the end of the century (IPCC, 2014).

60 Research on microorganisms facing climatic changes is scarce compared to that on animals
61 and plants (Cavicchioli et al., 2019; Dutta and Dutta, 2016; Reinold et al., 2019). Microbial
62 mats play important key-roles in marine ecosystems, such as participating in the dynamics of
63 carbon, nitrogen et oxygen cycles. They develop at the water-sediment interface in a large
64 variety of environments including coastal beaches (Bolhuis and Stal, 2011), salterns
65 (Fourçans et al., 2004), hot springs (Dobretsov et al., 2011) and many other coastal/marine
66 environments. These are complex microbial structures containing a great diversity of
67 microorganisms coexisting at microscale according to a vertical stratification due to light and
68 microgradients of oxygen, pH and sulphurs (Fourçans et al., 2008; Jorgensen et al., 1983;
69 Revsbech et al., 1983; van Gemerden, 1993). Despite the stratification, microbial mats are
70 dynamic structures where the migration of microorganisms has been described according to
71 the diel cycle (Fourçans et al., 2008, 2006). Numerous interactions occurs in microbial mats
72 representing thus an ecosystem on its own (Reinold et al., 2019). Microbial mats have a
73 remarkable specific, metabolic and molecular diversity, making them highly adaptable to the
74 changing physico-chemical conditions of the environment (Fourçans et al., 2006) as well as
75 to contamination (Bordenave et al., 2008, 2004a, 2004b).

76 microorganisms are fundamental organisms in the functioning of microbial mats because
77 they are primary producers.

78 Autotrophic microorganisms are fundamental organisms in the functioning of microbial mats
79 because they are the major primary producers. They can be chemotroph such as some
80 Bacteroidetes but the major primary producers in photosynthetic microbial mats are the
81 phototrophic microorganisms (Sørensen et al., 2005). Among them, Cyanobacteria produce
82 organic carbon which is then decomposed in the successive lower layers by different
83 heterotrophs. They also secrete adhesive and protective extracellular polymeric substances
84 (EPS), that form a matrix around the cells (Decho, 1990; Fourçans et al., 2006; Hubas, 2018;
85 Wieland et al., 2003). This matrix is generally composed of sugars, proteins, extracellular
86 DNA and other molecules in smaller proportions (Fourçans et al., 2006; Hubas, 2018;

Wieland et al., 2003). However, the composition varies depending on the physiological state of the organisms, the specific diversity, the growth stage of the mat and the physico-chemical conditions of the environment (Decho and Moriarty, 1990; Hubas, 2018; Reinold et al., 2019; Underwood et al., 2004). By binding to sedimentary particles, this matrix stabilises the microbial mat and prevents erosion phenomena (Decho, 1990), but it has many other essential roles such as nutrients supply by the sequestration and accumulation of dissolved and particulate nutrients coming from the water column that can be used by microorganisms, or it also helps microbial communication, or bring a protection against UV radiations (Decho, 2000; Flemming and Wingender, 2010; Hubas, 2018). EPS are therefore a major component of microbial mats and remain indispensable for their functioning.

Several studies have addressed the impact of climate change on photosynthetic marine microbial communities. Some authors have shown that temperature affects the composition, the photosynthetic performance as well as the growth, biomass and physiology of microphytobenthos (Cartaxana et al., 2015; Hancke and Glud, 2004). Acidification effects are thought to occur mainly at the metabolic level, favouring the growth of some microorganisms (Baragi and Anil, 2016; Black et al., 2019; Hicks et al., 2011) but also photorespiration in diatoms and increasing the number of proton pumps for maintaining intracellular pH homeostasis and respiratory processes (Beardall et al., 2009; Black et al., 2019; Gao et al., 2012). Acidification and warming also affect the characteristics of EPS of diatoms and cyanobacteria with a modification of their composition (Li et al., 2016; Ma et al., 2019).

Many studies have highlighted the impact of acidification and warming water separately but it is necessary to consider them together as they can act synergistically (Baragi et al., 2015; Baragi and Anil, 2016; Li et al., 2016). The aim of this study was to simulate an acidification and a water warming on microbial mats on mesocosms according to the RCP8.5 scenario of the IPPC for 2100. Here, the phototrophic microbial communities are described and their potential composition variation will be monitored.

2. Material and methods

2.1 Description of the sampled sites

Microbial mats for mesocosms experiment were sampled the 30th April 2019 in salterns located in Ars-en-Ré (46°13'29.9"N 1°31'07.5"W, Ré island, France) on a non-exploited pond. The microbial mat, which had not been disturbed for at least three years, was more mature than a mat from an exploited pond. Undisturbed mats were then placed in plastic boxes and transported to laboratory at room temperature where they were put back in water within three hours following the sampling. The water height was around 3 cm as observed *in situ*. *In situ* physico-chemical parameters (temperature, salinity, pH) of the water were measured with a multi-parameter probe (pHenomenal® MU 6100H, VWRTM, USA) in order to apply them on the mesocosms as control values. Samples were also taken to determine nutrient salt concentrations in the pore water.

2.2 Mesocosm design

Microbial mats were separated into twenty-four plastic boxes (48 cm x 33 cm), each of them representing a mesocosm (Fig. 1). The mesocosms were gathered in groups of six representing a condition (five replicates and a box for pulse amplitude modulated (PAM) measures). In these six mesocosms, incoming water was from a reserve and was distributed individually with stainless steel taps. This water corresponded to seawater filtered at 80 µm, passed under UV light and whose salinity was adjusted to 60 psu with salt coming the salt marshes of the Ré island. Opposite to the water inlet, a hole allowed the water outlet in a network of PVC tubes between all the replicates. The water was not recycled. This setup permitted to maintain a stable water level at 3 cm above the mat and to renew seawater and the supplying nutrients for the development of the microbial mats. For each condition, a pool was constructed around the six plastic boxes where water was maintained at the desired temperature with a pump (EHEIM universal 600, Germany) connected to a thermoregulating

device (Teco®) to control the water temperature above the microbial mats. The microbial mats were illuminated twelve hours a day following the day/night cycle observed during the spring. To control the evaporation rate, the lights used were LED (TOP-24H company by SYLED, France). They provided white cold light color and an intensity of $11.8 \pm 0.9 \mu\text{mol.photons.m}^{-2}.\text{s}^{-1}$ (mean \pm standard between the four treatments for a day) (HOBO Pendant® Temperature/Light Data Logger, Onset Computer Corporation, USA) on the surface of the microbial mats.

Daily monitoring was done for the physico-chemical parameters (temperature, pH, salinity and dissolved oxygen) thanks to a multiparameter probe (pHenomenal® MU 6100H, VWR™, USA).

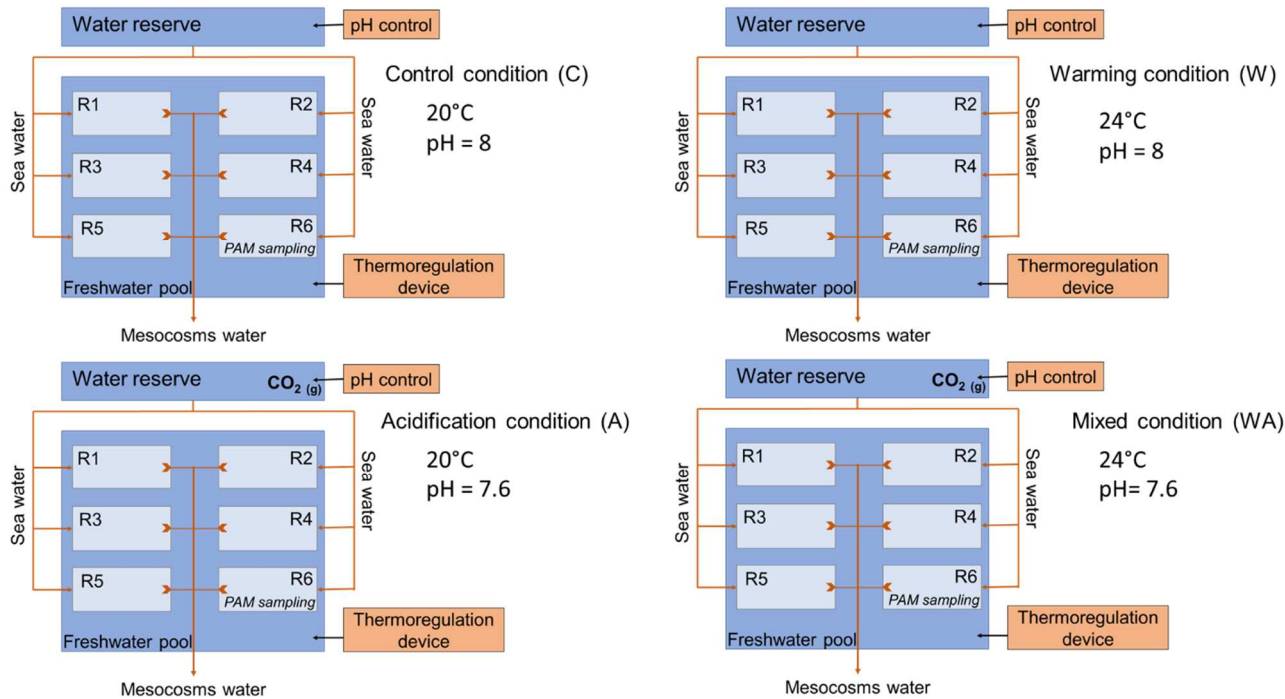


Figure 1: Schematic representation of the experimental device with the control (C) and the acidification (A), warming (W) and mixed (WA) treatments. The replicates are represented by the letter R, the first five are used for sampling and the sixth is dedicated to the measurements of fluorimetry by pulse amplitude modulation (PAM).

2.3 Implementation of different treatments

A stabilisation period of five weeks was applied to acclimate the microbial mats to their new environment (Gette-Bouvarot et al., 2015; Stauffert et al., 2013). The water temperature on

160 the mesocosms was maintained at 20°C and the salinity of the incoming water was regulated
161 in the water reserve to maintain a salinity at 60 +/- 2 psu in the mesocosms, reproducing *in*
162 *situ* conditions. The implementation of different treatments occurred for seven additional
163 weeks.

164 Four treatments were applied to the microbial mats. Each pool and its six mesocosms
165 represented a condition. The first treatment was the control treatment (C) in which the
166 parameters were not changed. The second treatment was the warming treatment (W) in
167 which the temperature was increased by 0.5°C every two days for 2 weeks until reaching
168 24°C. The acidification treatment (A) represented the third condition. The water acidification
169 was performed in the water reserve by bubbling pure CO₂, allowing a drop of initial water pH
170 of 0.1 unit every four days for 2 weeks until reaching a decrease of the initial pH of the water
171 reserve equal to 0.4 unit, *i.e.* 7.6. The water pH in the water reserve was monitored with a
172 continuous pH stat system (IKS aquastar, iks ComputerSysteme GmbH, Germany). Then the
173 pH values of the pH stat system were adjusted twice a week from measurement using a pH
174 meter (Metrohm, 826 pH mobile) with a glass electrode (Metrohm, electrode plus) calibrated
175 on the total scale using Tris buffer solution (provided by Andrew Dickson, Scripps Institution
176 Oceanography, San Diego). Every day, the pH values in the four treatments pools were also
177 measured on the total scale. The fourth treatment combined warming and acidification
178 treatments (WA). The mesocosms were then maintained under these treatments for 5 further
179 weeks.

180 A first sampling (noted t₉) was performed after the stabilisation period of the microbial mats
181 on the mesocosms, just before changing the environmental conditions. A second sampling
182 (t₁₆) was performed at the middle of the period of change and a third (t₂₃) at the end
183 (Supplementary materials, fig. A). After this period, sampling was performed every week (t₃₀,
184 t₃₇, t₄₄, t₅₁ and t₅₈) (Supplementary materials, fig. A). For each sampling, ten 1 cm depth
185 cores were collected with a 1 cm diameter cut-off syringe in each mesocosm and mixed
186 together in order to obtain a homogeneous sample.

2.4 Nutrient concentrations

A volume of 20 mL of water from each mesocosm was filtered at 0.22 μm in order to perform a nutrient analysis. The same was done for *in situ* samples. Half of the volume was frozen at -20°C while the other half was kept at 4°C for silicon analysis. The samples were then analyzed as described by Aminot and K  rouel (2007). Silicon, nitrate, nitrite and phosphate were measured by Segmented Continuous Flow Colorimetry (SFA) while ammonium was measured by SFA fluorimetry on an auto-analyser (SEAL AutoAnalyzer 3, SEAL analytical) (Aminot and K  rouel, 2007).

2.5 Photosynthetic parameters

Chlorophyll fluorescence parameters were measured at 5 different locations of the core using a fluorometer (Monitoring Pen, MP 100-E, Photon Systems Instruments, Czech Republic) illuminated with a blue LED emitter (455 nm). The samples were placed in the dark (for 5 min) before the measurement of Light Response Curves. Manufacturer predetermined LC3 protocol was used following manufacturer instructions. LC3 protocol was characterised by 7 steps of increasing light intensities (10, 20, 50, 100, 300, 500, 1000 $\mu\text{mol.photon.m}^{-2}.\text{s}^{-1}$) with an illumination duration of 60s. Minimum fluorescence level F_0^5 (Jesus et al., 2006) was obtained by using a non actinic measuring light pulse (30 μs , 900 $\mu\text{mol.photon.m}^{-2}.\text{s}^{-1}$), which induced the minimal chlorophyll fluorescence (F_0^5). The samples were then subjected to a saturating light pulse (2,400 $\mu\text{mol.photon.m}^{-2}.\text{s}^{-1}$). This made it possible to measure the maximum fluorescence level F_m^5 (Jesus et al., 2006). All measurement were done in the same conditions and at the same time.

The data was then downloaded from the device to a computer using FluorPen software (v1.0.6.1, Photon Systems Instruments, Czech Republic) and all calculations and analyses were performed using R.Studio software (version 4.0.3   RStudio, Inc.). From the measured parameters the effective quantum yields of photosynthesis ($\phi(\text{II})^5$) were calculated (Jesus et

al., 2006) (Equation 1). They indicate the community's maximum potential for photosynthetic activity.

$$\phi(II)^5 = \frac{F_m^5 - F_0^5}{F_m^5} \quad (\text{Equation 1})$$

2.6 Pigment identification and quantification

Lipophilic pigments were analyzed by high performance liquid chromatography (HPLC). Microbial mats were incubated with 95% methanol (buffered with 2% ammonium acetate) during 15 min, at -20°C in the dark. Extracts were then filtered with 0.2µm PTFE syringe filters and analyzed within 16h using an Agilent 1260 Infinity HPLC composed of a quaternary pump (VL 400 bar), a UV–VIS photodiode array detector (DAD 1260 VL, 190–950 nm), a fluorescence detector (FLD 1260 excitation: 425 nm, emission: 655 nm), and a 100µl automatic sample injector refrigerated at 4°C in the dark. Chromatographic separation was carried out using a C18 column for reverse phase chromatography (Supelcosil, 25 cm long, 4.6 mm inner diameter). The solvents used were: 0.5M ammonium acetate in methanol and water (85:15, v:v), acetonitrile and water (90:10, v:v), and 100% ethyl acetate. The solvent gradient was set according to Brotas and Plante-Cuny (2003), with a 0.5 mL min⁻¹ flow rate. Identification and calibration of the HPLC peaks were performed with ββ-carotene, canthaxanthin, chlorophyll *a*, chlorophyll *b*, chlorophyll *c*2, diatoxanthin, diadinoxanthin, fucoxanthin and pheophytin *a* standards. We identified all detected peaks by their absorption spectra and relative retention times using the Agilent OpenLab software. Quantification was performed using standard calibration curves built with repeated injections of standards over a range of dilutions. Xanthophylls, carotens and chlorophyll *b* and *c* were quantified at 470 nm, chlorophyll *a* and their derivatives as well as pheopigments were quantified at 665 nm. The relative abundance of each pigment (%) was calculated from its respective concentration in the sample (µg.mg⁻¹).

2.7 Extracellular Polymeric Substances (EPS) characterization

In a 15 mL Falcon® tube, 5 mL of microbial mat was mixed with an equivalent volume of seawater obtained by mixing water from the five sampled replicate and filtered at 0.22 µm for each treatment. The tubes were subjected to mechanical agitation by vortexing and by inversion at a rate of 40 oscillations.min⁻¹ for 1 h at 4°C in the dark. Then they were centrifuged at 3500 g for 10 min at 4°C. The supernatant, containing the colloidal fraction, was recovered and stored at -20°C while the pellet, containing the bound fraction, was resuspended in 5 mL of seawater (again obtained by mixing water from the five sampled replicate and filtered at 0.22 µm for each treatment). 1 g of Dowex resin (Dowex Marathon C, Na⁺, Sigma-Aldrich), was prepared according to the protocol of Takahashi *et al.* (2009). The tubes were again subjected to the same protocol to obtain the supernatant containing the fraction of bound EPS was recovered and stored at -20°C.

The carbohydrate dosage was performed according to Dubois' colorimetric method (Dubois *et al.*, 1956) while the protein dosage was performed according to the BiCinchoninic acid Assay (BCA) method using the Pierce™ Protein Assay Kit (Thermoscientific). A range of glucose (L-(-)-Glucose, 98%, Sigma-Aldrich) from 0 to 3 g.L⁻¹ and a range of bovine serum albumin (BSA) from 0 to 1 g.L⁻¹ were performed in seawater from the Ré island hypersalinated at 60 psu and filtered at 0.22 µm. For carbohydrates, 100 µL of EPS sample were placed in a tube, then 100 µL of 5% phenol (Solid Phenol, Sigma-Aldrich, France) and 500 µL of 98% sulphuric acid (Sulphuric Acid 98%, Carlo-Erba Reagents, France) were added. The tubes were incubated for 30 min in the dark and at room temperature. A volume of 200 µL of the standard range and each triplicate sample was deposited in a 96-well microplate (Falcon® 96-well Clear Microplat, Thermo Fisher Scientific). The absorbance of each well was measured at 490 nm with a spectrophotometer (SPECTROstar® Nano, BMG LAB). For proteins, 225 µL of reagent was prepared and stored in the dark at room temperature during the assay period. The assays were performed in 96-well microplates (Falcon® 96-well Clear Microplat, Thermo Fisher Scientific). 200 µL of reagents were placed in the wells and 25 µL standards or

triplicate samples were added. The microplates were incubated for 30 min at 37°C, then the absorbance of each sample was measured at 562 nm by a spectrophotometer (SPECTROstar® Nano, BMG LAB). Two calibration curves were drawn from the standard ranges and their respective abundances (corrected according to the kit indications for the BSA range), averaged over the duration of the experiment. They made it possible to determine the carbohydrate and protein concentrations. The latter were then related to the dry mass of the microbial mat.

To determine the dry mass of the microbial mat, a volume of 30 mL of microbial mat was collected and weighed to obtain the fresh mass (M_F). The sample was then freeze-dried to remove water from the sample (Lyophilisateur Christ Alpha 1-4, Grosseron, France) and reweighed to obtain the freeze-dried mass (M_L).

2.8 Data analysis

All calculations and analyses were performed on R.Studio software (version 4.0.3® RStudio, Inc.). The mean of physico-chemical parameters, the carbohydrates and proteins concentrations of each fraction and the photosynthetic parameters of each treatment were compared with each other at each sampling time. The normality and homoscedasticity of the data were previously verified by carrying out a Shapiro test and a Bartlett test respectively. If both conditions were met, the data were subjected to an analysis of variances (ANOVA). Otherwise, a Welch ANOVA was performed in the case of non-homogeneity of variances and a Kruskal-Wallis rank sum test in the case of non-normal data. If these tests were found to be significant ($p < 0.05$), then a pairwise comparison was performed using a Tukey test following the ANOVA, a Games-Howell test following a Welch ANOVA or a Nemenyi test following the Kruskal-Wallis test.

A Between Class Analysis (BCA) combined with hierarchical cluster analysis with a Bray dissimilarity index and ward.D2 method was done on pigments proportions.

3. Results

3.1 Efficiency of the physico-chemical changes

As expected, the temperature in W and WA treatments increased well by 4°C from the initial temperature, the one maintained in C and A treatments ($23.89 \pm 0.49^{\circ}\text{C}$; $23.82 \pm 0.48^{\circ}\text{C}$; $20.32 \pm 0.36^{\circ}\text{C}$; $20.23 \pm 0.48^{\circ}\text{C}$; respectively) (Fig. 2, A; Supplementary materials, fig. B). There was a delay of one week before reaching this increase after the change of state because this was the time needed to heat up all the water in the pool and then the mesocosms.

The pH of C and W treatments were stabilized after t37 at 7.94 ± 0.15 and 7.95 ± 0.09 , respectively (Fig.2, B; Supplementary materials, fig. B). The pH of A and WA treatments decreased until t44, then remaining stable at pH 7.87 ± 0.13 and 7.86 ± 0.10 , respectively (Fig.2, B; Supplementary materials, fig. B). No significant difference between the four treatments was found at t9 (Kruskal, $p > 0.05$).

The salinity (Fig. 2, C; Supplementary materials, fig. B) of C and A treatments remained stable at 60.87 ± 1.44 psu and 61.91 ± 1.79 psu, respectively. The salinity of the W treatment increased to a maximum mean value of 75.87 ± 4.84 psu after 40 days of incubation, and then decreased again to a final value of 67.35 ± 4.24 psu. The salinity of the WA treatment increased and reached its maximum value of 71.94 ± 6.55 psu on day 23 of the experiment and then decreased and remained at 66.13 ± 2.56 psu.

Dissolved oxygen remained stable between each treatment up to t16 (mean \pm standard deviation; 0.95 ± 1.18 mg.L⁻¹ for control, 0.61 ± 1.15 mg.L⁻¹ for pH, 0.60 ± 0.46 mg.L⁻¹ for W and 0.30 ± 0.24 mg.L⁻¹ for WA) (Fig. 2, D; Supplementary materials, fig. B). From t23, the dissolved oxygen of the treatments increased linearly to t58 with a slope of 0.07 day⁻¹ ($R^2 = 0.45$, Student-test, $p < 0.05$) for A, 0.05 day⁻¹ ($R^2 = 0.39$, Student-test, $p < 0.05$) for W and 0.03 day⁻¹ ($R^2 = 0.19$, Student-test, $p < 0.05$) for WA. The A treatment had a final oxygen concentration of 5.95 ± 1.63 mg.L⁻¹, significantly higher (ANOVA, $p < 0.05$) than that of the

other mesocosms by a factor of 1.6 for W, 2.2 for C and 2.4 for WA (mean \pm standard deviation).

The nutrients were analyzed thanks to the Redfield ratio calculations (Redfield, 1958). Only seven samples showed nitrogen limitation, notably four replicates of the A treatment at t30 and some samples showed a limitation of silicon (Supplementary materials, fig. B and C). Most of the samples showed phosphate limitation, but such phosphate limitation was also observed *in situ* (Supplementary materials, fig. B and C).

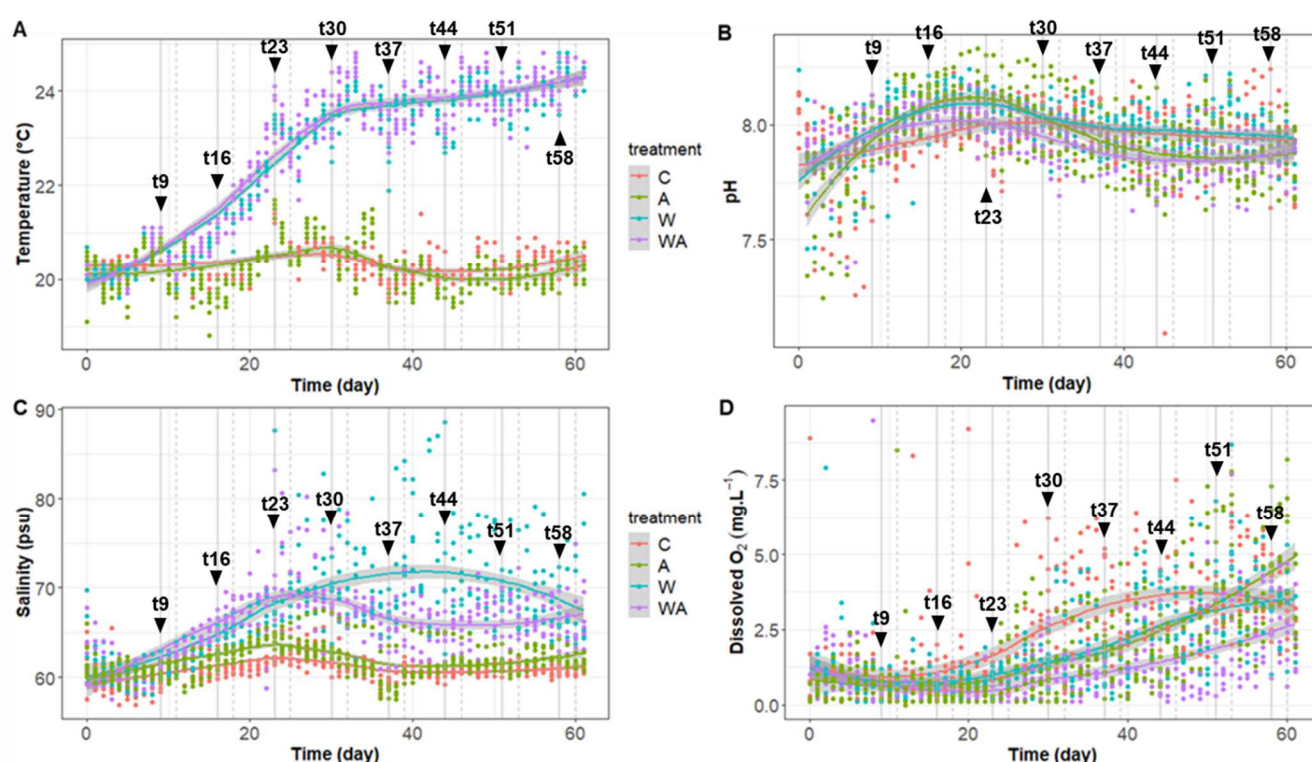


Figure 2: Temporal variation of the temperature (°C) (A), the pH (upH) (B), the salinity (psu) (C) and the dissolved oxygen (mg.L⁻¹) (D) of the different treatments (control (C), acidification (A), warming (W) or warming and acidification mix (WA)). The points corresponded to the values measured for each sample. The curves represented local regressions, based on the k-nearest neighbors algorithm (*geom_smooth* function of the *ggplot2* package, loess method). The grey areas symbolised the 95% confidence intervals. The sampling days were represented by black arrows. The day 0 to day 8 corresponded to the stabilisation week.

3.2 Pigment composition

A total of 37 pigments were identified. The analysis revealed the presence of several chlorophyll: chlorophyll *a* (Ca) and corresponding epimers and allomers, chlorophyll *b* (Cb)

and chlorophyll *c2* (Cc2). Bacteriochlorophyll *a* (BCa) was identified as well as echinenone, oscillol diquinovoside, myxol quinovoside and zeaxanthin. Other pigments were identified including lutein, alloxanthin, carotenoids and canthaxanthins and its isomers. Pigments corresponding to alteration products were also found: pyropheophytin, pheophytin *a*, pheophorbide *a* and chlorophyllide *a*. The presence of non-identified chlorophyll *a*-like molecules was also observed and hereby called chlorophyll derivatives (C deriv. #1-6).

Table 1: Pigments identified by HPLC and its corresponding abbreviations.

Pigment	Notation
alpha and beta Cryptoxanthin	aCy; bCy
Alloxanthin	Al
Beta-beta caroten; beta-epsilon caroten	BB.Car; BE.Car
Unknown carotenoids	Car1; Car2
Chlorophyll <i>a</i> ; Chlorophyll <i>a</i> allomers/epimers	Ca; Ca.allo; Ca.epi
Chlorophyll derivatives	C deriv. #1-6
Bacteriochlorophyll <i>a</i>	BCa
Chlorophyll <i>b</i>	Cb
Chlorophyll <i>c2</i>	Cc2
Chlorophyllide <i>a</i>	Cda
Canthaxanthin	Ct; Ct.iso
Echinenone	Ec
Fucoxanthin and isomers	F; F.iso1
Lutein and isomers	L; L.iso1; L.iso2
Myxol quinovoside and isomers	My.iso1; My.iso2; My.iso3; My.iso4
Oscillol diquinovoside	O
Pheophorbide	Pda.1
Pheophytin	Pha
Pyropheophytin	Pya
Zeaxanthin	Z

3.3 Acidification changes the pigments dynamics

At t9, all treatments were placed under the same water temperature and pH. No difference between pigments were observed (Fig.3) (ANOVA or Welch or Kruskal, $p>0.05$).

The C treatment was different from the other treatments containing more myxol quinovoside and isomers 2 and 3 than A treatment at t37 and t44 (Kruskal, $p<0.05$) and than the three other treatments at t51 (ANOVA, $p<0.05$). It also contained more chlorophyll epimers at t58 than A, W and WA treatments (ANOVA, $p<0.05$) (Fig.3). The W treatment was differentiated from the A treatment with the presence of chlorophyll derivative #6 at t51 and t58 (Welch,

356 $p < 0.05$) (Fig.3). The concentration of chlorophyll *a* was around 4% at the beginning of the
357 experiment (Fig. 4, A). It increased until t51 in all treatments except for A treatment and then
358 decreased at t58 (Fig. 4, A). The A treatment slightly decreased at t58 and the proportion of
359 chlorophyll *a* was lower in this treatment than in the C treatment (ANOVA, $p < 0.05$) at t51
360 and t58 (Fig. 4, A). Conversely, the proportion of chlorophyll derivatives (Fig. 4, B) was close
361 to 0 at t9 for all treatments. It increased to t30, remained stable at t44 and then decreased
362 again to t58 for the C, W and WA groups, while it increased to t44 before decreasing again to
363 t58 for the A group (Fig. 4, B). The proportion of chlorophyll derivatives was significantly
364 higher for the A treatment at t37, t44 and t51 (ANOVA and Welch, $p < 0.05$) (Fig. 4, B).

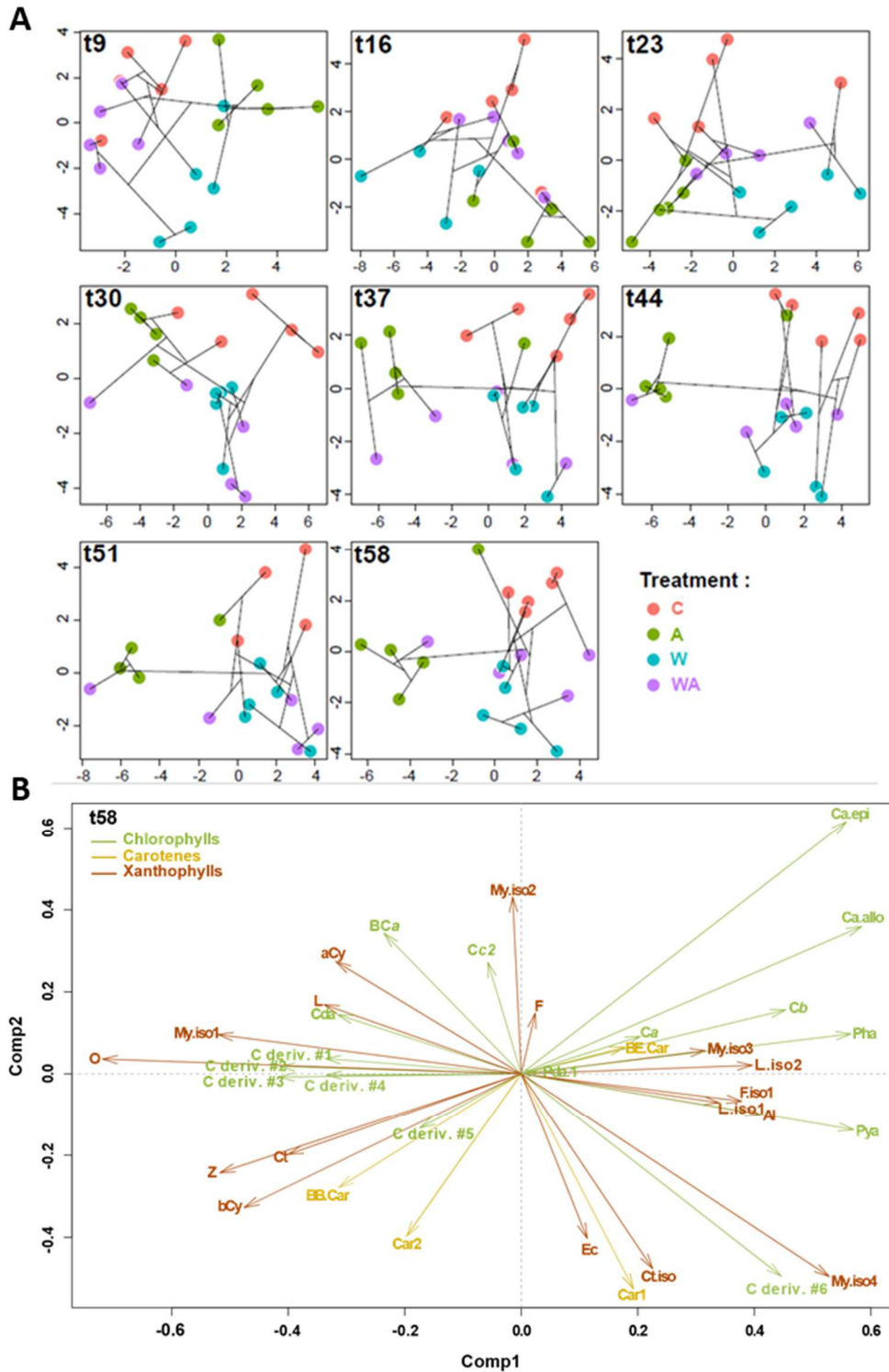


Figure 3: Dynamics of microbial communities according to pigments composition and the sampling time (tX) **(A)**. This figure was obtained thanks to analyze BCA combined with hierarchical cluster analysis with a Bray dissimilarity index and ward.D2 method. A representation more detailed with the different parameters was done at t58 **(B)**. The correspondence between the abbreviations and the names of pigments is provided on the **table 1**.

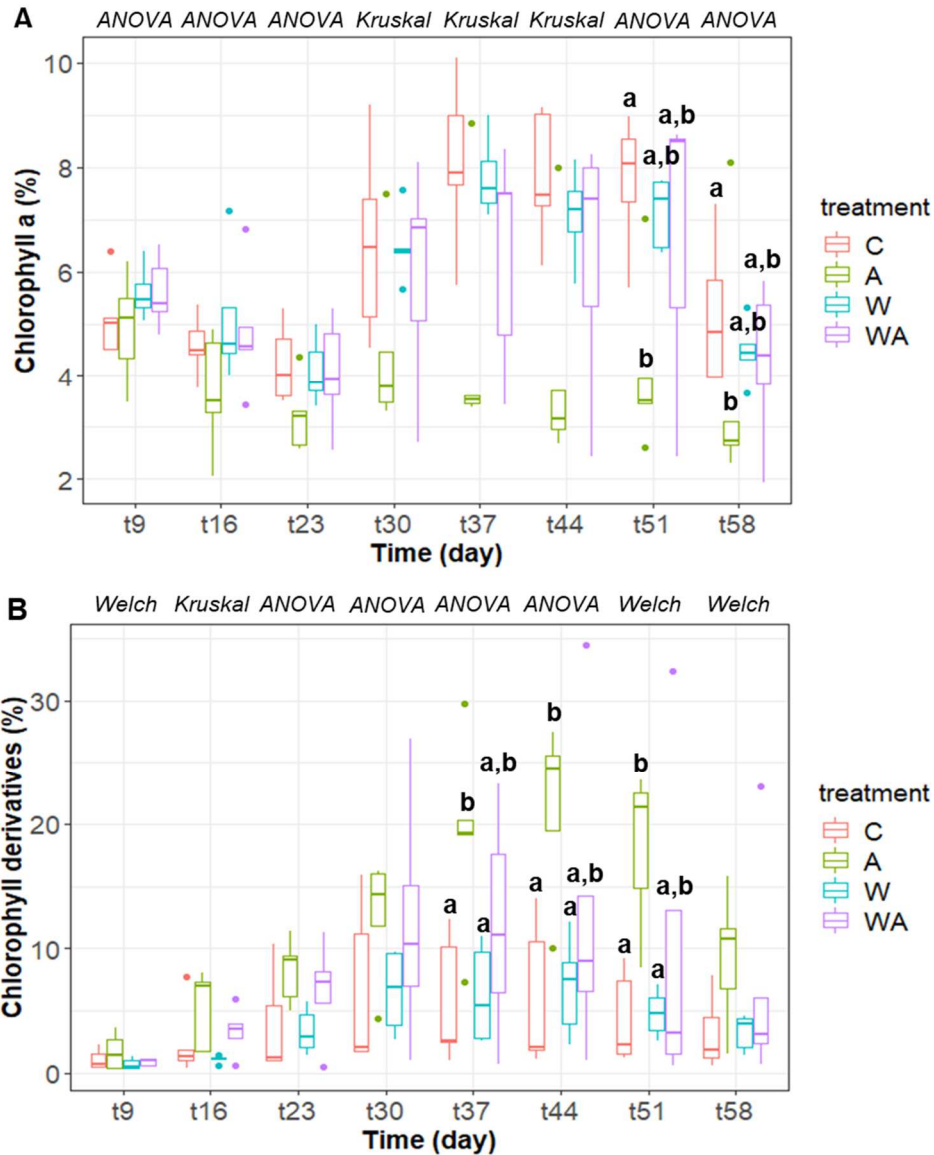
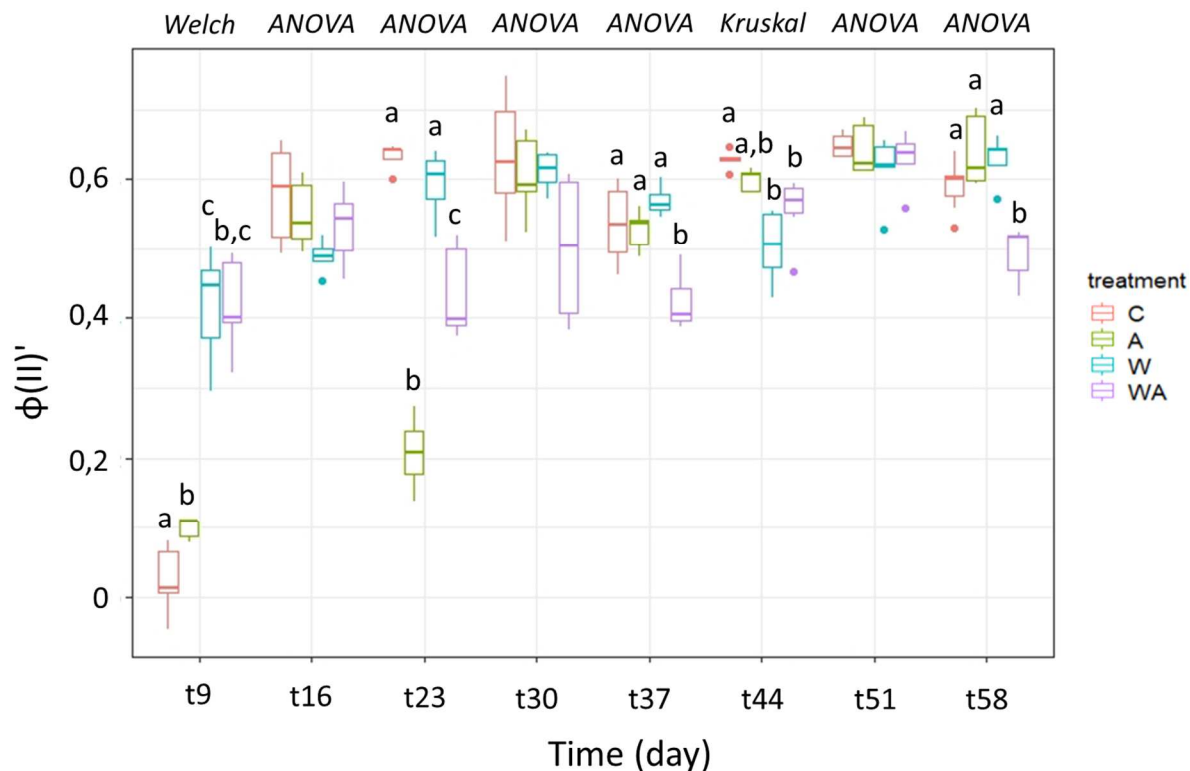


Figure 4: Temporal variations of **(A)** the concentration of chlorophyll a (%) and **(B)** the concentration of chlorophyll derivatives (%). The letters t followed by a number indicates the sampling time. The statistical test performed to show the differences between treatments at a sampling time is indicated in italics above the figure. The letters indicated a significant difference ($p < 0.05$) found after a post-hoc Tuckey test in the case of an ANOVA or a Games-Howell test in the case of a Welch ANOVA.

3.4 Comparison of the photosynthetic yields of the microbial mat in the different treatments

The quantum efficiency of photosystem II ($\phi(II)'$) indicated the photosynthetic efficiency of the mat. At t9, the quantum yields of the C and A treatments were close to 0, while those of the

W and WA groups were 14 and 4.2 times more than C and A treatments respectively (Fig. 5). At t16 no significant difference was observed between all the quantum yields (ANOVA, $p > 0.05$) (Fig. 5). Other difference were observed between treatments during the experiment, but the kinetics obtained showed no real trend between treatments (Fig. 5), only WA treatment presented a quantum yields lower than C treatment at t37, t51 and t58 (ANOVA or Kruskal, $p < 0.05$) than W and A treatments at t37 and t58 (ANOVA, $p < 0.05$).



392

Figure 5: Variation of the quantum efficiency of photosystem II ($\phi(II)'$) in the different treatment. The letters t followed by a number indicates the sampling time. Above the figure was indicated in italics the test carried out for the comparison between treatments of the same week. The letters indicated a significant difference ($p < 0.05$) found after a post-hoc Tukey HSD test in the case of an ANOVA, a Games-Howell test in the case of a Welch ANOVA or a Nemenyi test in the case of a Kruskal Wallis test.

399

3.5 Acidification impacted the proportion of EPS

401

The A treatment was dissimilar from the other treatments, characterized by its higher concentrations of bound carbohydrates EPS.

403

The carbohydrates bound EPS concentration was notably more important in A treatment on three times: at t23, t37 and t58 (ANOVA, $p < 0.05$) (Fig. 6).

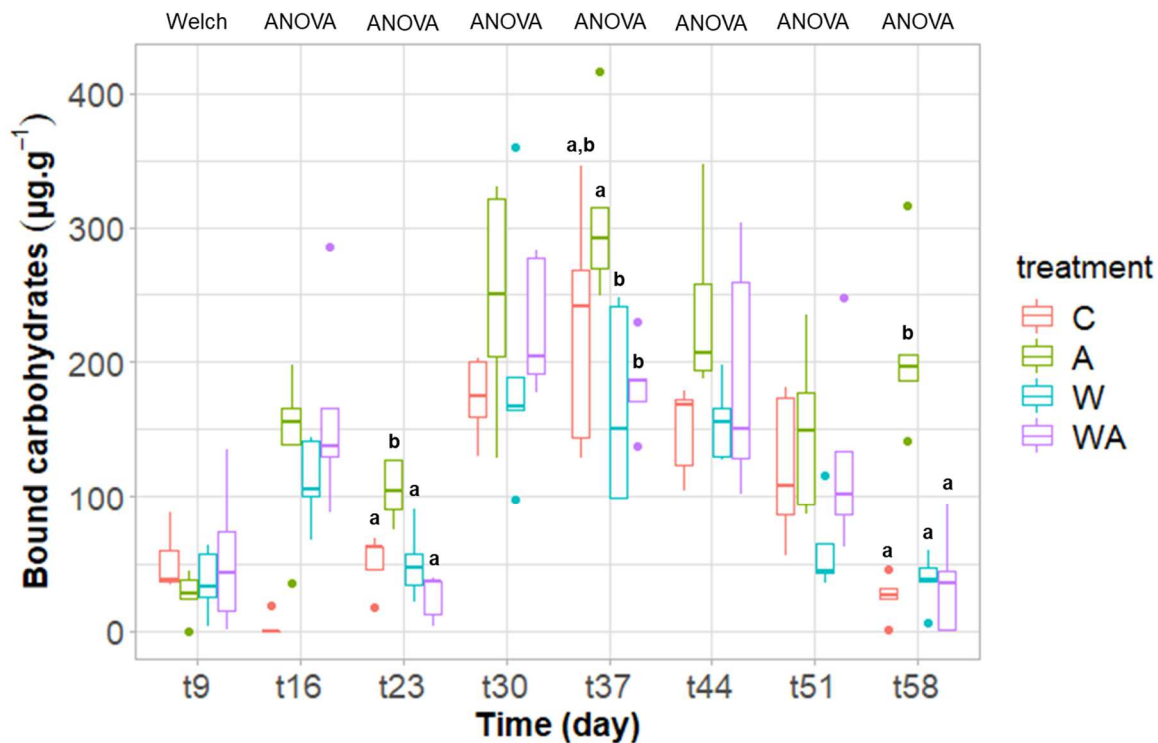


Figure 6: Temporal variation of the carbohydrate concentration in the bound fraction of EPS (in $\mu\text{g.g}^{-1}$ dry mass). The letters t followed by a number indicates the sampling time. The statistical test performed to show the differences between treatments at a sampling time is indicated in italics above the figure. The letters indicate a significant difference ($p < 0.05$) found after a post-hoc Tukey test. Note: the ANOVA performed at t16 did not consider the C treatment because of the presence of outliers.

4. Discussion

The aim of the study was to simulate acidification and/or warming on microbial mats. The mesocosm system has the advantage to control the physico-chemical parameters allowing to simulate future conditions, which is impossible to achieve directly in the field; but the natural environment can never be mimicked perfectly (weather, daily or even seasonal variations in physico-chemical parameters, *etc.*). Although mesocosm system will never faithfully represent reality, it is a compromise often used to conduct experimental ecology studies (Cravo-Laureau and Duran, 2014). It is therefore advisable to remain vigilant so as not to

423 extrapolate too generally the results obtained with *in situ* microbial mats. Given the diversity
424 of structure and functioning of microbial mats throughout the world, they may act differently in
425 their natural environment. It should also be noted that this study was a simulation of the
426 IPCC's most pessimistic predictions (RCP8.5) for 2100. The changes simulated only
427 concerned the decrease in water pH and the increase in water temperature, but these are
428 not the only parameters that are expected to vary in the future. Deoxygenation of the oceans,
429 a succession of extreme weather events, and sea level rise in some regions are also
430 foreseeable changes that have not been tested in this study. Moreover, they have been
431 monitored over seven weeks, whereas variations in the natural environment are supposed to
432 occur over several decades.

433 The renewal water in the mesocosm permitted to maintain a stable water level at 3 cm above
434 the mat and a natural supply of nutrients for the development of microbial mats. Redfield
435 ratio showed some limitation of nitrogen and/or phosphorus in the water under some
436 conditions but previous studies have shown that microbial mats can develop in P- (Peimbert
437 et al., 2012) and N-limited environment (Peimbert et al., 2012) (Supplementary materials, fig.
438 C).

439 Surprisingly, the decrease of pH under the A and WA treatments was not noticeable in the
440 mesocosms (Fig. 2) although the pH in the respective water reserve decreased
441 (Supplementary materials, fig. D) at the expected pH 7.6 (the initial pH was 8). This
442 phenomenon has been observed in other studies (Crawford et al., 2011; Ma et al., 2019).
443 The most likely hypothesis is that the rate of CO₂ fixation by photosynthesis was higher in the
444 A and WA treatments, which had the effect of increasing the pH. In our experiment, dissolved
445 oxygen increased under A treatment after the third week. Moreover, many microbial species
446 are able to use carbon concentration mechanisms (CCMs), storing high CO₂ concentrations
447 before transport into the Rubisco compartments, which minimise photorespiration. These
448 CCMs are found in oxygenic phototrophs like cyanobacteria or most of the phytoplankton
449 (Ma et al., 2019). The CCMs have been proposed as mechanisms to prevent photosynthetic

450 systems to directly detect ambient changes in CO₂ (Mackey et al., 2015). As a result,
451 photosynthetic rates might not respond directly to ambient changes in CO₂ explaining the
452 delay observed in the increase of dissolved oxygen in our experiment. Such observation is
453 consistent with the fact that pH decreased from t23 while dissolved oxygen continued to
454 increase (Fig. 2). Black et al. (2019) suggested that microphytobenthos use additional CO₂
455 due to acidification for photosynthesis until the maximum yield capacity has been reached.
456 When the cells reached maximum intracellular CO₂ concentration through their CCMs, any
457 additional CO₂ would contribute to the decrease in pH. The pH of the WA treatment followed
458 the same dynamic as observed for the A treatment. However, the dissolved oxygen
459 concentration under WA treatment increased less than half in comparison to the A treatment
460 (Fig. 2, D). The CO₂ absorption mechanisms may have been less efficient in WA treatment
461 because temperature decreases the solubility of CO₂ (Wootton et al., 2008).

462 Numerous studies have shown that photosystem II is very sensitive to environmental stress
463 (Murata et al., 2007; Nishiyama et al., 2008; Wang et al., 2013). It is therefore important to
464 focus on the quantum yield of photosystem II, which indicates the maximum photosynthetic
465 activity potential of the communities. At t9, the quantum yield of photosystem II for the C and
466 A treatments were close to 0 (Fig. 5), which indicated that the mats were not in good
467 physiological condition when starting the experiment. Significantly lower quantum yields were
468 observed under some treatments. At t23, under the A and the WA treatments an unexplained
469 decrease of the quantum yield was observed (Fig. 5). The WA treatment exhibited
470 significantly lower quantum yield than the other treatments at t37, t51 and t58 (Fig. 5),
471 suggesting that mats have more difficulty withstanding simultaneous acidification and
472 heating. It was not surprising that there was no difference in quantum efficiency between A
473 and C treatments (Fig. 5). Photosynthetic organisms have a high capacity to modify pH with
474 evidence that pH is regulated at the water/cell interface (Black et al., 2019). Our fluorometer
475 illuminated with a blue LED emitter (455 nm). Chlorophyll *a* fluorescence per unit
476 concentration in cyanobacteria tends to be lower than in algae when it is excited with blue

477 light. This leads to an erroneous biomass estimate of cyanobacteria. In their study, Simis *et*
478 *al.* (2012) have sought the optimal excitation and emission pairs for the separation of
479 cyanobacterial and algal Fv/Fm in communities. They demonstrate that the highest
480 correlation between community and cyanobacterial variable fluorescence is obtained under
481 orange-red excitation in the 590–650 nm range, exciting cyanobacterial phycobilipigments.
482 No information was found about the other phototrophic communities.

483 The A treatment possessed more chlorophyll derivatives and lower chlorophyll *a* than the
484 other treatments (Fig. 4). These chlorophyll derivatives molecules seemed to be bioindicators
485 of a stress condition (water acidification). They were not identified by available standards.
486 These molecules did not correspond to known metallised allomers or epimers of chlorophyll
487 *a* (Ca), as revealed by their retention time (Supplementary materials, fig. E). Based on their
488 absorption spectra (Fig. 7), we can also rule out the hypothesis that these molecules
489 correspond to de-metallised derivatives of chlorophyll *a* such as pheophytin *a* or
490 pheophorbide *a* or even to bacteriochlorophyll *a* (BCa).

491 We can assume that these molecules correspond to transmetalated Ca or BCa. Some
492 microorganisms are known to possess bacteriochlorophyll those the central Mg ion is
493 replaced by another metal, as observed for *Acidiphilium* where BCa possess a Zn central
494 metal (Hiraishi and Shimada, 2001). This organism has been isolated from acidic mine ponds
495 and it is supposed likely that pH constituted the evolutionary pressure responsible for the
496 change of the central metal (Hiraishi and Shimada, 2001). Although this is an attractive
497 hypothesis, it is highly unlikely that our pH treatment had the effect of promoting the
498 synthesis of transmetalated BCa as Zn-BCa displays absorption features in the near infra-red
499 range (Nagata *et al.*, 2003) that were not observed here.

500 Chlorophylls and porphyrin derivatives generally have two major absorption bands (*i.e.* “red”
501 (Q-) and “blue” (Soret-) bands, Fig. 7) in the visible range, due to extended π -delocalization
502 at the edge of cyclic porphyrin skeleton (Milenković *et al.*, 2012). Two main Q-bands ($Q_{y,0-0}$
503 and $Q_{y,0-1}$) are traditionally observed in the original Ca (or Mg-Ca) (Gerola *et al.*, 2011). In our

504 case, Ca wavelengths of maximum absorption λ_{\max} were respectively 665 ($Q_{y,0-0}$) and 615 nm
505 ($Q_{y,0-1}$).

506 Based on these findings, the unidentified derivatives do not correspond to transmetalated
507 Ca, although those absorption characteristics are close to the Mg-Ca molecule. As shown
508 previously by Gerola *et al.* (2011), a hypsochromic (blue) shift of both Soret and $Q_{y,0-0}$ bands
509 must be expected with significant decreasing of λ_{\max} in Zn- and Cu-Ca in comparison to Mg-
510 Ca. Such hypsochromic shifts were not observed in the unidentified derivatives spectra.

511 The only noticeable change corresponded to a decreased intensity (hypochromic effect) in
512 the $Q_{y,0-0}$ band in comparison with that of Mg-Ca and a bathochromic (red) shift in the $Q_{y,0-1}$.
513 (Fig.7). These characteristics are similar to those of bacteriochlorophyll *c* (BC*c*) with a
514 recorded λ_{\max} (630 nm) for $Q_{y,0-1}$ close to the expected 623-629 nm (Goedheer, 1966; Oelze,
515 1985; Pierson and Castenholz, 1974). This pigment is typically found in the chlorosomes of
516 green anoxygenic phototroph bacteria, including the green sulfur bacteria and the green non-
517 sulfur bacteria (Frigaard *et al.*, 2006; Scheer, 2006), which indicated that the pH conditions
518 may have favoured the growth of these phototrophic bacteria.

519 Even moderate changes of both pH and temperature are relevant for bacterial community
520 composition of microbial mats (Uribe-Lorío *et al.*, 2019). A decrease in chlorophyll *a* has
521 been observed under high CO₂ levels suggesting that the CO₂ input reduce CCMs and thus
522 save energy, particularly in pigment synthesis (Wang *et al.*, 2019; Yue *et al.*, 2019). In hot
523 springs from Costa Rica, significant changes of microbial mat communities were observed
524 with a significant increase of Chloroflexi (also named the green non-sulfur bacteria)
525 abundance with decreasing pH and increasing temperature (Uribe-Lorío *et al.*, 2019).
526 Chloroflexi have been previously reported to be more abundant at decreased pH on
527 sediment of hydrothermal CO₂ seeps in Papua New Guinea (Hassenrück *et al.*, 2016) and in
528 host-association with corals and sponges (Kandler *et al.*, 2018; Morrow *et al.*, 2015).
529 Chlorobi, the green sulfur bacteria, have also been found to increase in abundance with
530 acidification (Hassenrück *et al.*, 2016). On their study, Hassenrück *et al.* (2016) supposed

that in the sites characterized by low pH and high hydrothermal influence, including pronounced temperature increases, the Chloroflexi and Chlorobi replaced other microbial communities as major carbon degraders under anoxic conditions. Green anoxygenic bacteria participate on the carbon cycling and have been shown to fix CO₂ (Hug et al., 2013; Sirevåg, 2004). The phototrophic communities of the microbial mats could be modified under A treatment leading to a higher relative abundance of green anoxygenic bacteria. It is also possible that the presence of more CO₂ on the environment conducted to a shift on the metabolism of green anoxygenic phototrophic bacteria fixing the CO₂ and being more competitive with the other communities.

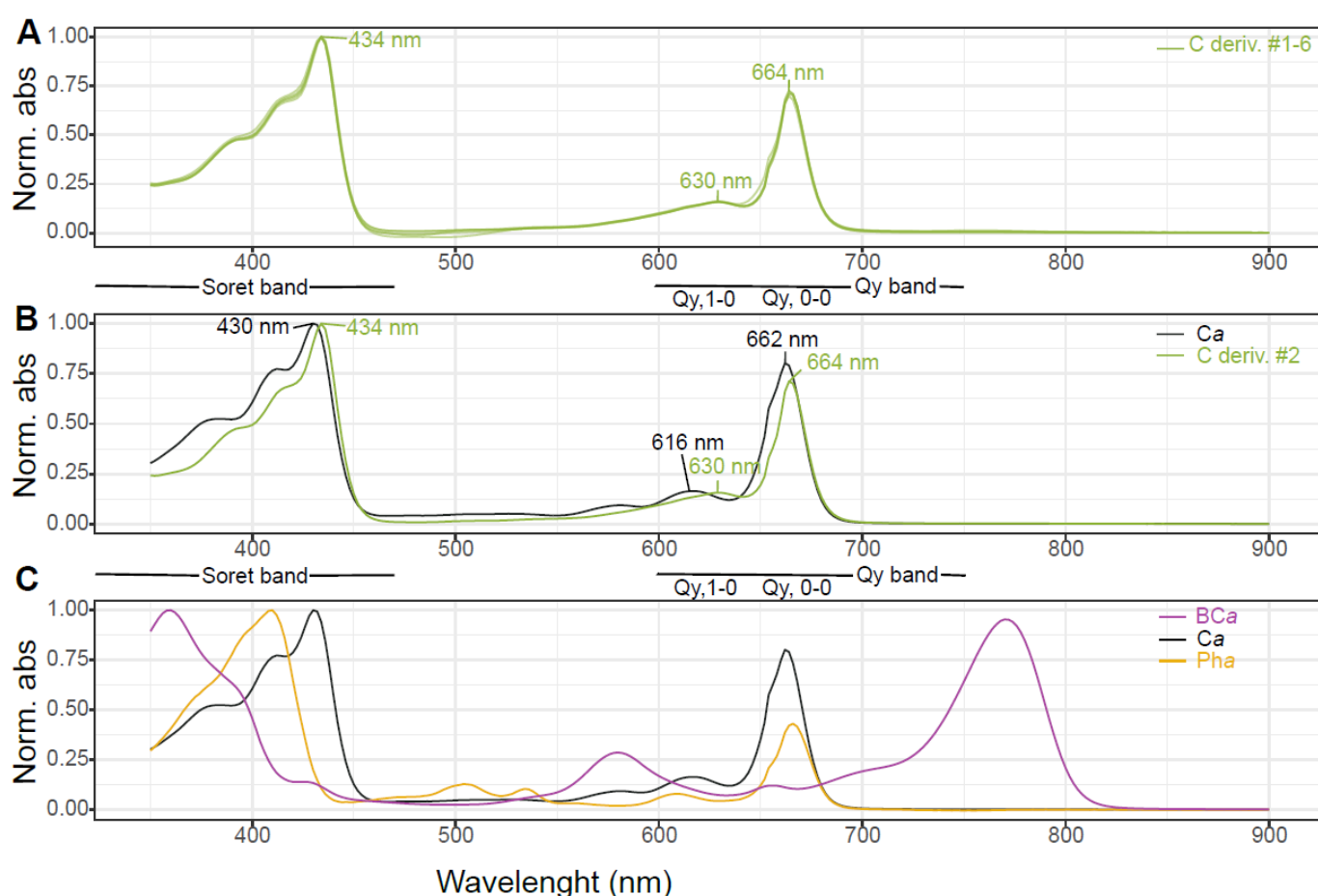


Figure 7: Normalized absorption spectra of different pigments of the microbial mats. **A:** superimposed absorption spectra of the 6 detected chlorophyll derivatives (C deriv.). **B:** comparison between the absorption spectra of chlorophyll a (Ca) and C deriv. #2. **C:**

comparison between the absorption spectra of Ca, pheophytin a (Pha) and bacteriochlorophyll a (BCa).

The bound carbohydrate EPS production was higher under the A treatment. EPS are essential for maintaining the physical properties and proper functioning of microbial mats, and are also involved in the adaptation of communities to their environment (Dupraz and Visscher, 2005; Hubas, 2018; Prieto-Barajas et al., 2018). Therefore, EPS are an essential element, even more when microorganisms are confronted with strong variations in physico-chemical parameters. It has been observed that the degradation of polysaccharides by bacterial extracellular enzymes is accelerated at low pH (Piontek et al., 2009). It can be supposed that microbial mats could therefore synthesize more carbohydrates to compensate for this degradation. Microbial mats in the W treatment did not show any variation in concentration, suggesting that temperature has no effect on this process. Those in the WA treatment also did not change suggesting that acidification and warming have probably antagonistic effects limiting the impact of acidification on EPS. However, Li *et al.* (2016) obtained contradictory results on three freshwater microalgae as they demonstrated that acidification and warming act synergistically. The variation of bound carbohydrate EPS suggest that microbial mats subjected to acidification modified their metabolism. Tan *et al.* (2019) have shown that a polar strain of *Chlorella sp.* modulates its metabolism under acidified conditions ($p\text{CO}_2 = 1000 \mu\text{atm}$), favouring its survival. They observed a decrease in the fluxes of glucose and sucrose, the main products of photosynthesis, under high $p\text{CO}_2$. Gong *et al.* (2020) also observed that the starch metabolism was modified by increasing the quantity of starch granules in another microalgae named *Symbiochlorum hainanensis*. These observations suggest that the organic carbon produced by photosynthesis in the microbial mats placed under the A treatment was redirected towards the synthesis of other carbohydrates which concentration had considerably increased.

5. Conclusion

573 The temperature in the warming treatments increased by 4°C from the initial temperature as
574 expected. Despite of a decrease of 0.4 unit pH in the water reserves of acidification
575 treatments, no significance difference was observed between the water pH of the different
576 treatments. The salinity increased on the warming treatments because of the water
577 evaporation. The dissolved oxygen concentration increased and was higher on the
578 acidification treatments, certainly due to an increase of the photosynthesis because of the
579 carbon input.

580 In the acidification treatment, our results showed that the concentration of bound
581 carbohydrates EPS increased. This indicated that the metabolisms were modified to cope
582 with the induced changes. In addition, the phototrophic communities of the microbial mats
583 under the different treatments showed characteristic pigments. In particular, unknown
584 chlorophyll derivatives were present under acidification and/or warming treatments. To the
585 best of our knowledge the synthesis of such derivatives following an acidification or/and a
586 warming experiment has never been reported before. These molecules were eventually
587 identified as bacteriochlorophyll *c* and several possible isomers which suggest that
588 experimentally induced climate change scenario may have favoured the increase of BC*c*
589 contained on green anoxygenic phototroph bacteria.

590 The mesocosm experiment has shown that phototrophic communities of the microbial mats
591 were able to adapt to the conditions defined by the IPCC (2014) regarding acidification and
592 warming of surface water. The most probable explanation is that the studied microbial mats
593 are already naturally confronted with environmental conditions (pH, light, temperature,
594 salinity, *etc.*) that fluctuate with a great amplitude in salt marshes. They may therefore
595 already be confronted with temperature and pH conditions predicted, for example, by the
596 IPCC for 2100. Changes in their metabolism probably enabled them to maintain a high
597 potential for photosynthetic activity when acidification took place. In the future, it would be
598 interesting to observe if a difference in the phylogenetic composition of these communities
599 occurred. This study provides new insights on the response of phototrophic communities of

microbial mats in a context of climatic change and permit to better understand their function in this ecosystem.

Acknowledgements

C. Mazière was supported by a PhD grant from E2S-UPPA program and the Région Nouvelle-Aquitaine. We thank the funding support from the European programme ERANETMED AQUASALT (NMED-0003-01) and from the ACI politique d'établissement Université de La Rochelle.

The authors are grateful to the salterns owner Michel Jauffrais and Thomas Lacoue-Labarthe for his help in setting up the acidification treatment.

References

- Aminot, A., Kérouel, R., 2007. Dosage automatique des nutriments dans les eaux marines., Quae. ed.
- Baragi, L.V., Anil, A.C., 2016. Synergistic effect of elevated temperature, pCO₂ and nutrients on marine biofilm. *Mar. Pollut. Bull.* 105, 102–109.
<https://doi.org/10.1016/j.marpolbul.2016.02.049>
- Baragi, L.V., Khandeparker, L., Anil, A.C., 2015. Influence of elevated temperature and pCO₂ on the marine periphytic diatom *Navicula distans* and its associated organisms in culture. *Hydrobiologia* 762, 127–142. <https://doi.org/10.1007/s10750-015-2343-9>
- Beardall, J., Stojkovic, S., Larsen, S., 2009. Living in a high CO₂ world: Impacts of global climate change on marine phytoplankton. *Plant Ecol. Divers.* 2, 191–205.
<https://doi.org/10.1080/17550870903271363>
- Black, J.G., Stark, J.S., Johnstone, G.J., McMinn, A., Boyd, P., McKinlay, J., Wotherspoon, S., Runcie, J.W., 2019. In-situ behavioural and physiological responses of Antarctic microphytobenthos to ocean acidification. *Sci. Rep.* 9, 1890. <https://doi.org/10.1038/s41598-018-36233-2>
- Bolhuis, H., Stal, L.J., 2011. Analysis of bacterial and archaeal diversity in coastal microbial mats using massive parallel 16S rRNA gene tag sequencing. *ISME J.* 5, 1701–1712.
<https://doi.org/10.1038/ismej.2011.52>
- Bordenave, S., Fourçans, A., Blanchard, S., Goñi, M.S., Caumette, P., Duran, R., 2004a. Structure and functional analyses of bacterial communities changes in microbial mats following petroleum exposure. *Ophelia* 58, 195–203. <https://doi.org/10.1080/00785236.2004.10410227>
- Bordenave, S., Goñi-urriza, M., Vilette, C., Blanchard, S., Caumette, P., Duran, R., 2008. Diversity of ring-hydroxylating dioxygenases in pristine and oil contaminated microbial mats at genomic and transcriptomic levels. *Environ. Microbiol.* 10, 3201–3211.
<https://doi.org/10.1111/j.1462-2920.2008.01707.x>
- Bordenave, S., Jézéquel, R., Fourçans, A., Budzinski, H., Merlin, F.X., Fourel, T., Goñi-Urriza, M., Guyoneaud, R., Grimaud, R., Caumette, P., Duran, R., 2004b. Degradation of the “Erika” oil. *Aquat. Living Resour.* 17, 261–267. <https://doi.org/10.1051/alr:2004027>

639 Brotas, V., Plante-Cuny, M.-R., 2003. The use of HPLC pigment analysis to study microphytobenthos
640 communities. *Acta Oecologica* 24. [https://doi.org/10.1016/S1146-609X\(03\)00013-4](https://doi.org/10.1016/S1146-609X(03)00013-4)

641 Cartaxana, P., Vieira, S., Ribeiro, L., Rocha, R., Cruz, S., Calado, R., Marques da Silva, J., 2015. Effects
642 of elevated temperature and CO₂ on intertidal microphytobenthos. *BMC Ecol.* 15, 10.
643 <https://doi.org/10.1186/s12898-015-0043-y>

644 Cavicchioli, R., Ripple, W.J., Timmis, K.N., Azam, F., Bakken, L.R., Baylis, M., Behrenfeld, M.J., Boetius,
645 A., Boyd, P.W., Classen, A.T., Crowther, T.W., Danovaro, R., Foreman, C.M., Huisman, J.,
646 Hutchins, D.A., Jansson, J.K., Karl, D.M., Koskella, B., Mark Welch, D.B., Martiny, J.B.H.,
647 Moran, M.A., Orphan, V.J., Reay, D.S., Remais, J.V., Rich, V.I., Singh, B.K., Stein, L.Y., Stewart,
648 F.J., Sullivan, M.B., van Oppen, M.J.H., Weaver, S.C., Webb, E.A., Webster, N.S., 2019.
649 Scientists' warning to humanity: microorganisms and climate change. *Nat. Rev. Microbiol.* 17,
650 569–586. <https://doi.org/10.1038/s41579-019-0222-5>

651 Cravo-Laureau, C., Duran, R., 2014. Marine coastal sediments microbial hydrocarbon degradation
652 processes: contribution of experimental ecology in the omics'era. *Front. Microbiol.* 5.
653 <https://doi.org/10.3389/fmicb.2014.00039>

654 Crawford, K.J., Raven, J.A., Wheeler, G.L., Baxter, E.J., Joint, I., 2011. The Response of *Thalassiosira*
655 *pseudonana* to Long-Term Exposure to Increased CO₂ and Decreased pH. *PLoS ONE* 6,
656 e26695. <https://doi.org/10.1371/journal.pone.0026695>

657 Decho, A., 2000. Microbial biofilms in intertidal systems: an overview. *Cont. Shelf Res.* 20, 1257–
658 1273. [https://doi.org/10.1016/S0278-4343\(00\)00022-4](https://doi.org/10.1016/S0278-4343(00)00022-4)

659 Decho, A., 1990. Decho AW.. Microbial exopolymer secretions in ocean environments: their role(s) in
660 food webs and marine processes. *Oceanogr Mar Biol Ann Rev* 28: 73-153. *Oceanogr. Mar.*
661 *Biol. Annu. Rev.* 28, 73–154.

662 Decho, A.W., Moriarty, D.J.W., 1990. Bacterial exopolymer utilization by a harpacticoid copepod: A
663 methodology and results. *Limnol. Oceanogr.* 35, 1039–1049.
664 <https://doi.org/10.4319/lo.1990.35.5.1039>

665 Dobretsov, S., Abed, R.M.M., Al Maskari, S.M.S., Al Sabahi, J.N., Victor, R., 2011. Cyanobacterial mats
666 from hot springs produce antimicrobial compounds and quorum-sensing inhibitors under
667 natural conditions. *J. Appl. Phycol.* 23, 983–993. <https://doi.org/10.1007/s10811-010-9627-2>

668 Dubois, Michel., Gilles, K.A., Hamilton, J.K., Rebers, P.A., Smith, Fred., 1956. Colorimetric Method for
669 Determination of Sugars and Related Substances. *Anal. Chem.* 28, 350–356.
670 <https://doi.org/10.1021/ac60111a017>

671 Dupraz, C., Visscher, P.T., 2005. Microbial lithification in marine stromatolites and hypersaline mats.
672 *Trends Microbiol.* 13, 429–438. <https://doi.org/10.1016/j.tim.2005.07.008>

673 Dutta, H., Dutta, A., 2016. The microbial aspect of climate change. *Energy Ecol. Environ.* 1, 209–232.
674 <https://doi.org/10.1007/s40974-016-0034-7>

675 Flemming, H.-C., Wingender, J., 2010. The biofilm matrix. *Nat. Rev. Microbiol.* 8, 623–633.
676 <https://doi.org/10.1038/nrmicro2415>

677 Fourçans, A., Oteyza, T.G. de, Wieland, A., Solé, A., Diestra, E., Bleijswijk, J. van, Grimalt, J.O., Köhl,
678 M., Esteve, I., Muyzer, G., Caumette, P., Duran, R., 2004. Characterization of functional
679 bacterial groups in a hypersaline microbial mat community (Salins-de-Giraud, Camargue,
680 France). *FEMS Microbiol. Ecol.* 51, 55–70. <https://doi.org/10.1016/j.femsec.2004.07.012>

681 Fourçans, A., Ranchou-Peyruse, A., Caumette, P., Duran, R., 2008. Molecular Analysis of the Spatio-
682 temporal Distribution of Sulfate-reducing Bacteria (SRB) in Camargue (France) Hypersaline
683 Microbial Mat. *Microb. Ecol.* 56, 90–100. <https://doi.org/10.1007/s00248-007-9327-x>

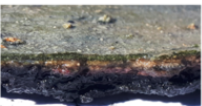
684 Fourçans, A., Solé, A., Diestra, E., Ranchou-Peyruse, A., Esteve, I., Caumette, P., Duran, R., 2006.
685 Vertical migration of phototrophic bacterial populations in a hypersaline microbial mat from
686 Salins-de-Giraud (Camargue, France). *FEMS Microbiol. Ecol.* 57, 367–377.
687 <https://doi.org/10.1111/j.1574-6941.2006.00124.x>

688 Frigaard, N.-U., Maqueo Chew, A.G., Maresca, J.A., Bryant, D.A., 2006. Bacteriochlorophyll
689 Biosynthesis in Green Bacteria, in: Grimm, B., Porra, R.J., Rüdiger, W., Scheer, H. (Eds.),

- Chlorophylls and Bacteriochlorophylls, *Advances in Photosynthesis and Respiration*. Springer Netherlands, Dordrecht, pp. 201–221. https://doi.org/10.1007/1-4020-4516-6_15
- Gao, K., Helbling, E., Häder, D., Hutchins, D., 2012. Responses of marine primary producers to interactions between ocean acidification, solar radiation, and warming. *Mar. Ecol. Prog. Ser.* 470, 167. <https://doi.org/10.3354/meps10043>
- Gerola, A.P., Tsubone, T.M., Santana, A., de Oliveira, H.P.M., Hioka, N., Caetano, W., 2011. Properties of Chlorophyll and Derivatives in Homogeneous and Microheterogeneous Systems. *J. Phys. Chem. B* 115, 7364–7373. <https://doi.org/10.1021/jp201278b>
- Gette-Bouvarot, M., Mermillod-Blondin, F., Lemoine, D., Delolme, C., Danjean, M., Etienne, L., Volatier, L., 2015. The potential control of benthic biofilm growth by macrophytes—A mesocosm approach. *Ecol. Eng.* 75, 178–186. <https://doi.org/10.1016/j.ecoleng.2014.12.001>
- Goedheer, J.C., 1966. Visible Absorption and Fluorescence of Chlorophyll and Its Aggregates in Solution, in: *The Chlorophylls*. Elsevier, pp. 147–184. <https://doi.org/10.1016/B978-1-4832-3289-8.50012-6>
- Gong, S., Jin, X., Xiao, Y., Li, Z., 2020. Ocean Acidification and Warming Lead to Increased Growth and Altered Chloroplast Morphology in the Thermo-Tolerant Alga *Symbiodinium hainanensis*. *Front. Plant Sci.* 11. <https://doi.org/10.3389/fpls.2020.585202>
- Hancke, K., Glud, R., 2004. Temperature effects on respiration and photosynthesis in three diatom-dominated benthic communities. *Aquat. Microb. Ecol.* 37, 265–281. <https://doi.org/10.3354/ame037265>
- Hassenrück, C., Fink, A., Lichtschlag, A., Tegetmeyer, H.E., de Beer, D., Ramette, A., 2016. Quantification of the effects of ocean acidification on sediment microbial communities in the environment: the importance of ecosystem approaches. *FEMS Microbiol. Ecol.* 92. <https://doi.org/10.1093/femsec/fiw027>
- Hicks, N., Bulling, M.T., Solan, M., Raffaelli, D., White, P.C., Paterson, D.M., 2011. Impact of biodiversity-climate futures on primary production and metabolism in a model benthic estuarine system. *BMC Ecol.* 11, 7. <https://doi.org/10.1186/1472-6785-11-7>
- Hiraishi, A., Shimada, K., 2001. Aerobic anoxygenic photosynthetic bacteria with zinc-bacteriochlorophyll. *J. Gen. Appl. Microbiol.* 47, 161–180. <https://doi.org/10.2323/jgam.47.161>
- Hubas, C., 2018. Biofilms, tapis et agrégats microbiens : vers une vision unificatrice (HDR (Habilitation à Diriger les Recherches)). Muséum National D'Histoire Naturelle. <https://doi.org/10.5281/zenodo.3784703>
- Hug, L.A., Castelle, C.J., Wrighton, K.C., Thomas, B.C., Sharon, I., Frischkorn, K.R., Williams, K.H., Tringe, S.G., Banfield, J.F., 2013. Community genomic analyses constrain the distribution of metabolic traits across the Chloroflexi phylum and indicate roles in sediment carbon cycling. *Microbiome* 1, 22. <https://doi.org/10.1186/2049-2618-1-22>
- Hutchins, D.A., Fu, F., 2017. Microorganisms and ocean global change. *Nat. Microbiol.* 2, 17058. <https://doi.org/10.1038/nmicrobiol.2017.58>
- IPCC, 2014. Climate Change 2014: Synthesis Report. Contribution of Working Groups I, II and III to the Fifth Assessment Report of the Intergovernmental Panel on Climate Change 169.
- Jesus, B., Perkins, R.G., Mendes, C.R., Brotas, V., Paterson, D.M., 2006. Chlorophyll fluorescence as a proxy for microphytobenthic biomass: alternatives to the current methodology. *Mar. Biol.* 150, 17–28. <https://doi.org/10.1007/s00227-006-0324-2>
- Jorgensen, B.B., Revsbech, N.P., Cohen, Y., 1983. Photosynthesis and structure of benthic microbial mats: Microelectrode and SEM studies of four cyanobacterial communities1. *Limnol. Oceanogr.* 28, 1075–1093. <https://doi.org/10.4319/lo.1983.28.6.1075>
- Kandler, N.M., Abdul Wahab, M.A., Noonan, S.H.C., Bell, J.J., Davy, S.K., Webster, N.S., Luter, H.M., 2018. In situ responses of the sponge microbiome to ocean acidification. *FEMS Microbiol. Ecol.* 94. <https://doi.org/10.1093/femsec/fiy205>

- Li, W., Xu, X., Fujibayashi, M., Niu, Q., Tanaka, N., Nishimura, O., 2016. Response of microalgae to elevated CO₂ and temperature: impact of climate change on freshwater ecosystems. *Environ. Sci. Pollut. Res.* 23, 19847–19860. <https://doi.org/10.1007/s11356-016-7180-5>
- Ma, J., Wang, P., Wang, X., Xu, Y., Paerl, H.W., 2019. Cyanobacteria in eutrophic waters benefit from rising atmospheric CO₂ concentrations. *Sci. Total Environ.* 691, 1144–1154. <https://doi.org/10.1016/j.scitotenv.2019.07.056>
- Mackey, K., Morris, J., Morel, F., Kranz, S., 2015. Response of Photosynthesis to Ocean Acidification. *Oceanography* 25, 74–91. <https://doi.org/10.5670/oceanog.2015.33>
- Milenković, S.M., Zvezdanović, J.B., Anđelković, T.D., Marković, D.Z., 2012. THE IDENTIFICATION OF CHLOROPHYLL AND ITS DERIVATIVES IN THE PIGMENT MIXTURES: HPLC-CHROMATOGRAPHY, VISIBLE AND MASS SPECTROSCOPY STUDIES. *Adv. Technol.* 9.
- Morrow, K.M., Bourne, D.G., Humphrey, C., Botté, E.S., Laffy, P., Zaneveld, J., Uthicke, S., Fabricius, K.E., Webster, N.S., 2015. Natural volcanic CO₂ seeps reveal future trajectories for host–microbial associations in corals and sponges. *ISME J.* 9, 894–908. <https://doi.org/10.1038/ismej.2014.188>
- Murata, N., Takahashi, S., Nishiyama, Y., Allakhverdiev, S.I., 2007. Photoinhibition of photosystem II under environmental stress. *Biochim. Biophys. Acta BBA - Bioenerg., Structure and Function of Photosystems* 1767, 414–421. <https://doi.org/10.1016/j.bbabi.2006.11.019>
- Nagata, M., Yoshimura, Y., Inagaki, J., Suemori, Y., Iida, K., Ohtsuka, T., Nango, M., 2003. Construction and Photocurrent of Light-harvesting Polypeptides/Zinc Bacteriochlorophyll *a* Complex in Lipid Bilayers. *Chem. Lett.* 32, 852–853. <https://doi.org/10.1246/cl.2003.852>
- Nishiyama, Y., Allakhverdiev, S.I., Murata, N., 2008. Regulation by Environmental Conditions of the Repair of Photosystem II in Cyanobacteria, in: Demmig-Adams, B., Adams, W.W., Mattoo, A.K. (Eds.), *Photoprotection, Photoinhibition, Gene Regulation, and Environment, Advances in Photosynthesis and Respiration*. Springer Netherlands, Dordrecht, pp. 193–203. https://doi.org/10.1007/1-4020-3579-9_13
- Oelze, J., 1985. 9 Analysis of Bacteriochlorophylls**Dedicated to Prof. Dr. N. Pfennig on the occasion of his 60th birthday in recognition of his numerous contributions on the ecology and taxonomy of phototrophic bacteria., in: Bergan, T. (Ed.), *Methods in Microbiology*. Academic Press, pp. 257–284. [https://doi.org/10.1016/S0580-9517\(08\)70478-1](https://doi.org/10.1016/S0580-9517(08)70478-1)
- Peimbert, M., Alcaraz, L.D., Bonilla-Rosso, G., Olmedo-Alvarez, G., García-Oliva, F., Segovia, L., Eguarte, L.E., Souza, V., 2012. Comparative Metagenomics of Two Microbial Mats at Cuatro Ciénegas Basin I: Ancient Lessons on How to Cope with an Environment Under Severe Nutrient Stress. *Astrobiology* 12, 648–658. <https://doi.org/10.1089/ast.2011.0694>
- Pierson, B.K., Castenholz, R.W., 1974. A phototrophic gliding filamentous bacterium of hot springs, *Chloroflexus aurantiacus*, gen. and sp. nov. *Arch. Microbiol.* 100, 5–24. <https://doi.org/10.1007/BF00446302>
- Piontek, J., Lunau, M., Händel, N., Borchard, C., Wurst, M., Engel, A., 2009. Acidification increases microbial polysaccharide degradation in the ocean. *Biogeosciences Discuss.* 7. <https://doi.org/10.5194/bg-7-1615-2010>
- Prieto-Barajas, C.M., Valencia-Cantero, E., Santoyo, G., 2018. Microbial mat ecosystems: Structure types, functional diversity, and biotechnological application. *Electron. J. Biotechnol.* 31, 48–56. <https://doi.org/10.1016/j.ejbt.2017.11.001>
- Rae, B.D., Long, B.M., Badger, M.R., Price, G.D., 2013. Functions, Compositions, and Evolution of the Two Types of Carboxysomes: Polyhedral Microcompartments That Facilitate CO₂ Fixation in Cyanobacteria and Some Proteobacteria. *Microbiol. Mol. Biol. Rev. MMBR* 77, 357–379. <https://doi.org/10.1128/MMBR.00061-12>
- Redfield, A.C., 1958. The biological control of chemical factors in the environment. *Am. Sci.* 46, 230A–221.
- Reinold, Wong, MacLeod, Meltzer, Thompson, Burns, 2019. The Vulnerability of Microbial Ecosystems in A Changing Climate: Potential Impact in Shark Bay. *Life* 9, 71. <https://doi.org/10.3390/life9030071>

792 Revsbech, N.P., Jorgensen, B.B., Blackburn, T.H., Cohen, Y., 1983. Microelectrode studies of the
 793 photosynthesis and O₂, H₂S, and pH profiles of a microbial mat¹. *Limnol. Oceanogr.* 28,
 794 1062–1074. <https://doi.org/10.4319/lo.1983.28.6.1062>
 795 Scheer, H., 2006. An Overview of Chlorophylls and Bacteriochlorophylls: Biochemistry, Biophysics,
 796 Functions and Applications, in: Grimm, B., Porra, R.J., Rüdiger, W., Scheer, H. (Eds.),
 797 Chlorophylls and Bacteriochlorophylls: Biochemistry, Biophysics, Functions and Applications,
 798 Advances in Photosynthesis and Respiration. Springer Netherlands, Dordrecht, pp. 1–26.
 799 https://doi.org/10.1007/1-4020-4516-6_1
 800 Sirevåg, R., 2004. Carbon Metabolism in Green Bacteria, in: Blankenship, R.E., Madigan, M.T., Bauer,
 801 C.E. (Eds.), Anoxygenic Photosynthetic Bacteria, Advances in Photosynthesis and Respiration.
 802 Kluwer Academic Publishers, Dordrecht, pp. 871–883. [https://doi.org/10.1007/0-306-47954-](https://doi.org/10.1007/0-306-47954-0_40)
 803 [0_40](https://doi.org/10.1007/0-306-47954-0_40)
 804 Sørensen, K.B., Canfield, D.E., Teske, A.P., Oren, A., 2005. Community Composition of a Hypersaline
 805 Endoevaporitic Microbial Mat. *Appl. Environ. Microbiol.* 71, 7352–7365.
 806 <https://doi.org/10.1128/AEM.71.11.7352-7365.2005>
 807 Stauffert, M., Cravo-Laureau, C., Jezequel, R., Barantal, S., Cuny, P., Gilbert, F., Cagnon, C., Milton, C.,
 808 Amouroux, D., Mahdaoui, F., Bouyssié, B., Stora, G., Merlin, F., Duran, R., 2013. Impact of
 809 Oil on Bacterial Community Structure in Bioturbated Sediments. *PloS One* 8, e65347.
 810 <https://doi.org/10.1371/journal.pone.0065347>
 811 Takahashi, E., Ledauphin, J., Goux, D., Orvain, F., 2009. Optimising extraction of extracellular
 812 polymeric substances (EPS) from benthic diatoms: Comparison of the efficiency of six EPS
 813 extraction methods. *Mar. Freshw. Res.* 60, 1201–1210. <http://dx.doi.org/10.1071/MF08258>
 814 Tan, Y.-H., Lim, P.-E., Beardall, J., Poong, S.-W., Phang, S.-M., 2019. A metabolomic approach to
 815 investigate effects of ocean acidification on a polar microalga *Chlorella* sp. *Aquat. Toxicol.*
 816 217, 105349. <https://doi.org/10.1016/j.aquatox.2019.105349>
 817 Underwood, G.J.C., Boulcott, M., Raines, C.A., Waldron, K., 2004. Environmental Effects on
 818 Exopolymer Production by Marine Benthic Diatoms: Dynamics, Changes in Composition, and
 819 Pathways of Production¹. *J. Phycol.* 40, 293–304. [https://doi.org/10.1111/j.1529-](https://doi.org/10.1111/j.1529-8817.2004.03076.x)
 820 [8817.2004.03076.x](https://doi.org/10.1111/j.1529-8817.2004.03076.x)
 821 Uribe-Lorío, L., Brenes-Guillén, L., Hernández-Ascencio, W., Mora-Amador, R., González, G., Ramírez-
 822 Umaña, C.J., Díez, B., Pedrós-Alió, C., 2019. The influence of temperature and pH on bacterial
 823 community composition of microbial mats in hot springs from Costa Rica. *MicrobiologyOpen*
 824 8. <https://doi.org/10.1002/mbo3.893>
 825 van Gernerden, H., 1993. Microbial mats: A joint venture. *Mar. Geol.* 113, 3–25.
 826 [https://doi.org/10.1016/0025-3227\(93\)90146-M](https://doi.org/10.1016/0025-3227(93)90146-M)
 827 Wang, S., Zhang, D., Pan, X., 2013. Effects of cadmium on the activities of photosystems of *Chlorella*
 828 *pyrenoidosa* and the protective role of cyclic electron flow. *Chemosphere* 93, 230–237.
 829 <https://doi.org/10.1016/j.chemosphere.2013.04.070>
 830 Wang, X., Feng, X., Zhuang, Y., Lu, J., Wang, Y., Gonçalves, R.J., Li, X., Lou, Y., Guan, W., 2019. Effects
 831 of ocean acidification and solar ultraviolet radiation on physiology and toxicity of
 832 dinoflagellate *Karenia mikimotoi*. *Harmful Algae* 81, 1–9.
 833 <https://doi.org/10.1016/j.hal.2018.11.013>
 834 Wieland, A., Köhl, M., McGowan, L., Fourçans, A., Duran, R., Caumette, P., Garcia de Oteyza, T.,
 835 Grimalt, J.O., Solé, A., Diestra, E., Esteve, I., Herbert, R.A., 2003. Microbial Mats on the
 836 Orkney Islands Revisited: Microenvironment and Microbial Community Composition. *Microb.*
 837 *Ecol.* 46, 371–390. <https://doi.org/10.1007/s00248-002-0108-2>
 838 Wootton, J.T., Pfister, C.A., Forester, J.D., 2008. Dynamic patterns and ecological impacts of declining
 839 ocean pH in a high-resolution multi-year dataset. *Proc. Natl. Acad. Sci.* 105, 18848–18853.
 840 <https://doi.org/10.1073/pnas.0810079105>
 841 Yue, F., Gao, G., Ma, J., Wu, H., Li, X., Xu, J., 2019. Future CO₂-induced seawater acidification
 842 mediates the physiological performance of a green alga *Ulva linza* in different photoperiods.
 843 *PeerJ* 7. <https://doi.org/10.7717/peerj.7048>



Control
20°C – pH = 8

Acidification treatment
20°C – pH =
7.6

Warming treatment
24°C – pH = 8

**Acidification +
warming treatment**
24°C – pH =
7.6

Photosynthetic efficiency	=	=	=	=
Extracellular polymeric substances	=	+ (bound carbohydrates EPS)	=	=
Chlorophyll a	=	-	=	=
Chlorophyll derivatives	=	+	=	=



Change in the phototrophic communities

OR

Change in the metabolism of green anoxygenic phototroph bacteria